pharmaceutics

MDPI

Article

Fluorescein-Labeled Thiacalix[4]arenes as Potential Theranostic Molecules: Synthesis, Self-Association, and Antitumor Activity

Alan Akhmedov [1,*], Olga Terenteva [1], Evgenia Subakaeva [2], Pavel Zelenikhin [2], Ramilia Shurpik [1], Dmitriy Shurpik [1], Pavel Padnya [1] and Ivan Stoikov [1,3,*]

[1] A.M. Butlerov Chemical Institute, Kazan Federal University, Kremlevskaya, 18, 420008 Kazan, Russia
[2] Institute of Fundamental Medicine and Biology, Kazan Federal University, Kremlevskaya, 18, 420008 Kazan, Russia
[3] Federal State Budgetary Scientific Institution, Federal Center for Toxicological, Radiation, and Biological Safety, Nauchny Gorodok-2, 420075 Kazan, Russia
* Correspondence: naive2294@gmail.com (A.A.); ivan.stoikov@mail.ru (I.S.); Tel.: +7-843-233-7463 (I.S.)

Abstract: In this paper, a series of thiacalix[4]arenes were synthesized as potential theranostic molecules for antitumor therapy. We propose an original strategy for the regioselective functionalization of thiacalix[4]arene with a fluorescent label to obtain antiangiogenic agent mimetics. The aggregation properties of the synthesized compounds were determined using the dynamic light scattering. The average hydrodynamic diameter of self-associates formed by the macrocycles in *1,3-alternate* conformation is larger (277–323 nm) than that of the similar macrocycle in *cone* conformation (185–262 nm). The cytotoxic action mechanism of the obtained compounds and their ability to penetrate into of human lung adenocarcinoma and human duodenal adenocarcinoma cells were established using the MTT-test and flow cytometry. thiacalix[4]arenes in *1,3-alternate* conformation did not have a strong toxic effect. The toxicity of macrocycles in *cone* conformations on *HuTu-80* and *A549* cells (IC_{50} = 21.83–49.11 μg/mL) is shown. The resulting macrocycles are potential theranostic molecules that combine both the pharmacophore fragment for neoplasmas treatment and the fluorescent fragment for monitoring the delivery and biodistribution of nanomedicines.

Keywords: thiacalixarene; antitumor activity; theranostics; fluorescein; quaternary ammonium salts; A549; HuTu-80

Citation: Akhmedov, A.; Terenteva, O.; Subakaeva, E.; Zelenikhin, P.; Shurpik, R.; Shurpik, D.; Padnya, P.; Stoikov, I. Fluorescein-Labeled Thiacalix[4]arenes as Potential Theranostic Molecules: Synthesis, Self-Association, and Antitumor Activity. *Pharmaceutics* **2022**, *14*, 2340. https://doi.org/10.3390/pharmaceutics14112340

Academic Editors: Irina Terekhova and Nataliya Kochkina

Received: 29 September 2022
Accepted: 26 October 2022
Published: 30 October 2022

1. Introduction

Cancer is a serious problem for modern society. In 2020, it is estimated that there were 19.3 million new cancer cases and nearly 10.0 million cancer deaths worldwide. New cases are forecast to reach 28.4 million in 2040, up 47% from 2020 [1]. Dysregulation of the immune response plays a significant role in the pathogenesis of cancer [2,3]. A number of mechanisms are known to allow tumor cells to form their microenvironment in order to suppress antitumor immunity [4,5]. One of these mechanisms is the tumor-associated production of galectins-1,3, which implement a wide range of extra- and intracellular functions [6–8]. Galectins-1,3 are involved in all stages of the tumor process [7]. Galectin-1 is a diagnostic marker of tumors [4], particularly tumors of the digestive tract (colon [9,10], liver [11,12], pancreas [13]), tumors of the respiratory system [14] and some lymphoid malignancies [15] and is also involved in angiogenesis and tumor growth [16].

In this regard, one of the modern types of anticancer drugs is galectin-1 inhibitors [17,18]. Increased drug resistance causes the overexpression of galectin-1 in malignant tumors; so-called multimodal therapy is used to combat this. Such multimodal therapy is an approach to cancer treatment that combines radiation and chemotherapy with several therapeutic methods [19]. Thus, multimodal therapy, including galectin-1 inhibitors, may increase the efficacy of co-administered drugs [17,18]. There are several different types of galectin-1

inhibitors, e.g., modified mono- and disaccharides containing galactose, or its analogs, non-carbohydrate-based inhibitors, such as peptides and peptidomimetics. The most successful peptide-based inhibitor of galectin-1 is anginex (*βpep-25*), a 33 amino acid peptide that exhibits antiangiogenic and antitumor effects [20].

Although anginex shows strong antitumor activity in vivo, non-peptide compounds are generally considered to be the preferred choice. Non-peptide compounds can potentially be administered orally without immune response and can also be optimized in terms of chemical and metabolic stability, resulting in better absorption and distribution to organs and tissues. Therefore, a series of topomimetics (calix[4]arene derivatives) based on anginex and partial peptidomimetics, taking into account the hydrophobic and hydrophilic fragments that are part of the anginex β-sheet, were synthesized [21]. Macrocycles **PTX008** and **PTX009** (Figure 1) have been identified as potent inhibitors of angiogenesis in cell proliferation and migration assays and in mouse models of ovarian cancer and melanoma [21,22]. This line of calixarene-based topomimetics has been patented by the Regents of the University of Minnesota as antibacterial, antiangiogenic, and antitumor agents, exhibiting the indicated activity in vitro and in vivo [23]. The mechanism of galectin-1 inhibition by calix[4]arene **PTX008** (Figure 1) was studied by HSQC spectroscopy, and it was shown that **PTX008** and anginex interact with galectin-1 through their hydrophobic surfaces [24]. In addition, a similar preparation based on the thiacalix[4]arene platform **PTX014** was obtained (Figure 1), and its antitumor activity was shown [22].

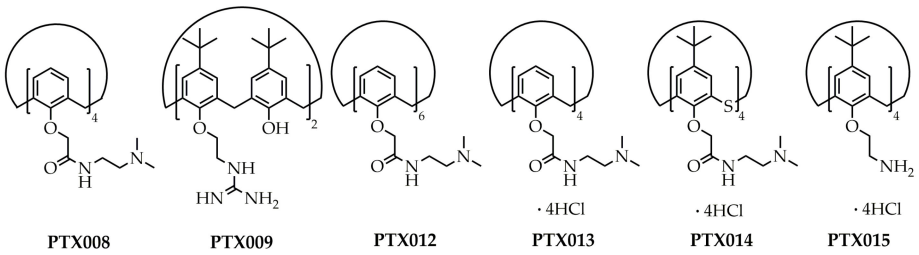

Figure 1. Calixarenes cytotoxic antitumor agents **PTX008**–**PTX015**.

Modern macrocyclic systems have demonstrated unprecedented advantages in the diagnosis and therapy of neoplastic diseases in recent years, using the advantages of supramolecular chemistry [25–43]. Highly specific detection and topical therapy are still the main targets for theranostic anticancer agents. We proposed the idea of combining the properties of an anticancer drug and a diagnostic agent in one molecule to create theranostic molecules. As a pharmacophore fragment, it was proposed to use macrocycles analogs of anti-angiogenic agents **PTX008**–**PTX015**, in which one of the substituents of the fragments is covalently functionalized with fluorescein. In this work, we developed an original strategy for the regioselective functionalization of the thiacalix[4]arene platform to obtain fluorescein-containing analogs of **PTX008**–**PTX015**. This approach makes it possible to create theranostic molecules that combine both the pharmacophore fragment for the treatment of tumor neoplasms and the fluorescent fragment for monitoring the delivery and biodistribution of nanomedicines. The mechanism of the cytotoxic action of the obtained compounds and their ability to penetrate into cancer cells of human lung adenocarcinoma (*A549*) and human duodenal adenocarcinoma (*HuTu-80*) were determined by the MTT test and flow cytometry.

2. Materials and Methods

2.1. Chemistry

All reagents and solvents (Sigma-Aldrich, St. Louis, MO, USA) were used directly as purchased or purified according to the standard procedures. The ^{1}H, ^{13}C and ^{1}H-^{1}H NOESY NMR spectra were recorded on an Avance 400 spectrometer (Bruker Corp., Billerica, MA, USA) (400 MHz for H-atoms) for 3–5% solutions in $CDCl_3$, DMSO-d_6. The residual solvent peaks were used as an internal standard. The FTIR ATR spectra were recorded

on the Spectrum 400 FT-IR spectrometer (Perkin Elmer, Seer Green, Lantrisant, UK) with a Diamond KRS-5 attenuated total internal reflectance attachment (resolution 0.5 cm^{-1}, accumulation of 64 scans, recording time 16 s in the wavelength range 400–4000 cm^{-1}). ESI HRMS experiments were performed at Agilent 6550 iFunnel Q-TOF LC/MS (Agilent Technologies, Santa Clara, CA, USA), equipped with Agilent 1290 Infinity II LC. Melting points were determined using the Boetius Block apparatus. Additional control of the purity of compounds and monitoring of the reaction were carried out by thin-layer chromatography using Silica G, 200 µm plates, UV 254.

*2.2. Synthesis of Compounds **4a–b**, **5a–d**, **6a–d***

Compounds **1** and **2** were synthesized according to published procedures [44–46]. Compounds **3a** and **3b** were synthesized according to published procedures. [45,47]

2.2.1. General Synthesis Procedure **4a–b**

Compound **3a** or **3b** (0.5 g, 0.43 mmol) and *N*,*N*-dimethylpropane-1,3-diamine (52.10 mmol) were mixed in a round-bottom flask equipped with a magnetic stirrer. In the case of **3b,** methanol (5 mL) was also added. The reaction mixture was stirred for 70 h at room temperature in the case of **3a**. The reaction mixture was stirred for 24 h at room temperature, followed by 46 h under cooling in the case of **3b**. Then, the solution was evaporated on a rotary evaporator, washed with water, and the residue was dried in a vacuum over phosphorus pentoxide. Products **4a–b** were obtained as a white powder. Characterizations of synthesized compounds **4a–b** are reported in the Supplementary Materials.

2.2.2. General Synthesis Procedure **5a–d**

A solution of 0.35 g (0.294 mmol) of compound **4a** (or **4b**) in DMF was prepared in a round-bottom flask equipped with a magnetic stirrer. Then, a solution of 0.324 mmol of the compound (FITC or PhIC) in DMF was added to the flask. The reaction mixture was stirred for 24 h at room temperature. The solution was evaporated on a rotary evaporator until DMF was partially removed. Then, 75 mL of the corresponding ether (MTBE in the case of FITC, Et_2O in the case of PhIC) was added to the resulting concentrated solution. A precipitate formed; it was washed with the appropriate ether, and the residue was dried in vacuum over phosphorus pentoxide. Products **5a–d** were obtained as bright orange or yellow powders. Characterizations of synthesized compounds **5a–d** are reported in the Supplementary Materials.

2.2.3. General Synthesis Procedure **6a–d**

A solution of 0.1 g (0.063 mmol) of compound **5a–d** in methanol was prepared in a round-bottom flask equipped with a magnetic stirrer. Then 0.1 mL (32 mol) of methyl iodide was added to the flask. The reaction mixture was stirred for 24 h at room temperature. The solution was evaporated on a rotary evaporator, and the residue was dried in vacuum over phosphorus pentoxide. Products **6a–d** were obtained as pale orange or yellow powders. Characterizations of synthesized compounds **6a–d** are reported in the Supplementary Materials.

2.3. Determination of the Hydrodynamic Particle Size by Dynamic Light Scattering

The particle size was determined by the Zetasizer Nano ZS instrument (Worcestershire, UK) at 25 °C. The instrument contains a 4 mW He-Ne laser operating at a wavelength of 633 nm and incorporated noninvasive backscatter optics (NIBS). The measurements were performed at the detection angle of 173°, and the software automatically determined the measurement position within the quartz cuvette. Synthesized compounds **6a–d** were dissolved completely in deionized water at concentrations used in the research (from 1×10^{-6} M to 1×10^{-3} M). Deionized water with resistivity >18.0 MΩ cm (Millipore-Q) was used for the preparation of the solutions.

*2.4. Cytotoxicity of **6a–d** on A549 and HuTu-80 Cell Lines*

The ability of macrocyclic compounds to inhibit the viability and proliferative activity of *A549* and *HuTu-80* cells was determined using the MTT assay according to [48]. Briefly, cells were grown in 96-well plates in DMEM (GIBCO, Waltham, MA, USA) after supplementing with 10% FBS (Corning Inc., Corning, NY, USA), 100 units/mL penicillin (PanEco, Moscow, Russia) and 100 μg/mL streptomycin (PanEco, Russia), at 37 °C in a humidified atmosphere with 5% CO_2 up to 80% confluence. Then, the medium in wells was replaced with a fresh medium, supplemented with test substances in the concentration range of 0.5–100 μg/mL. The volume of the culture medium in the wells was 100 μL. After 24 h of cell incubation in the presence of agents, the medium in the wells was replaced with a fresh medium containing MTT (Merck) at a concentration of 0.5 mg/mL. Cells were incubated with MTT for 3 h (*HuTu-80*) or 4 h (*A549*) at 37 °C, then the medium from the wells was aspirated and 100 μL of dimethyl sulfoxide added. Probes were incubated at 37 °C for 15 min in the dark for the formazan crystals to dissolve. The optical density of the formazan solution in the wells was measured using a reader (BioRad xMark™ Microplate Spectrophotometer, Hercules, CA, USA) at a wavelength of 570 nm. Three series of experiments were carried out with at least 8 replications for each variant in the series.

*2.5. Characterization of **6a–d** Penetration into A549 and HuTu-80 Cells by Flow Cytometry*

The macrocyclic compounds' ability to penetrate into *A549* and *HuTu-80* cells was determined with a BD FACSCanto II flow cytometer. Cells were incubated for 2 h in the presence of test compounds at 37 °C and then stained with propidium iodide (PI), which selectively stains dead cells.

A549 and *HuTu-80* cells were grown in DMEM (GIBCO, Waltham, MA, USA) after supplementing with 10% FBS (Corning, Inc., Corning, NY, USA), 100 units/mL penicillin (PanEco, Moscow, Russia) and 100 μg/mL streptomycin (PanEco, Moscow, Russia), at 37 °C in a humidified atmosphere with 5% CO_2. Cells were harvested and washed with fresh medium and then placed in individual sterile tubes at a concentration of 10^5 cells/mL. After adding the test compounds to the tubes, the cell suspension was incubated for 2 h at 37 °C in the dark. Then the cell suspension was centrifuged at 2000 rpm for 5 min at room temperature, and cells were washed three times in phosphate-buffered saline (PBS, PanEco, Moscow, Russia). The cells were resuspended in 1 mL of PBS and transferred to cytometric tubes, when the samples were stained with 5 μL of PI solution (5 mg/mL), kept in the dark at room temperature for 2 min, and cytometric analysis was performed. The processing of cytometric data was carried out in the FACSDiva application.

3. Results and Discussion

3.1. Synthesis of Fluorescein- and Phenyl-Labeled thiacalix[4]arenes

To develop an approach to the design of macrocyclic drugs containing a covalently attached fluorescent label, it was proposed to synthesize various lower-rim substituted thiacalix[4]arenes containing tertiary amino groups and fluorescein fragment. Monophthalimide **2** (Scheme 1) was proposed as a precursor for the synthesis of target differently substituted *p-tert*-butyl-thiacalix[4]arenes containing one fluorescent fragment [44]. At the first stage, compound **2** was synthesized according to the method of Ref. [44] (Scheme 1). It is known [44] that, regardless of the reaction conditions, the monosubstituted product **2** is formed in *cone* conformation, which opens up possibilities for further functionalization of the three unsubstituted hydroxyls. The formation of compound **2**, apparently, is a consequence of two factors, i.e., the use of a bulky substituent (phthalimide group), which shields the phenolic groups of the macrocycle, and the formation of intramolecular hydrogen bonds between the carbonyl groups of the phthalimide fragment and the phenolic hydroxyl groups of thiacalix[4]arene. Intramolecular hydrogen bonds (OH···O=C) fix the phthalimide substituent in a position that prevents the next molecule of the alkylating agent from approaching the reaction center [44,45]. Next, the alkylation reaction of derivative **2** with ethyl bromoacetate was carried out. An analysis of the literature data showed that the

alkylation of unsubstituted thiacalix[4]arene uses alkali metal carbonates as a template [49]. Thus, conformational stereoselectivity is easily controlled by selecting the appropriate alkali metal carbonate. In this case, the template effect is the main controlling factor. High selectivity is observed in acetone; the use of Na_2CO_3, K_2CO_3, and Cs_2CO_3 makes it possible to obtain *cone*, *partial cone*, and *1,3-alternate* in 77, 58, and 78% yields, respectively [49]. The template effect in acetone can be explained by the fact that the intermediate phenolate precursors are more closely coordinated with the template metal ions [49]. Alkylation of compound **2** with ethyl bromoacetate in acetone at the boiling point of the solvent for 80 h using sodium or cesium carbonates made it possible to obtain compounds **3b** [45] in *cone* conformation and **3a** [45] in *1,3-alternate* conformation, respectively (Scheme 1).

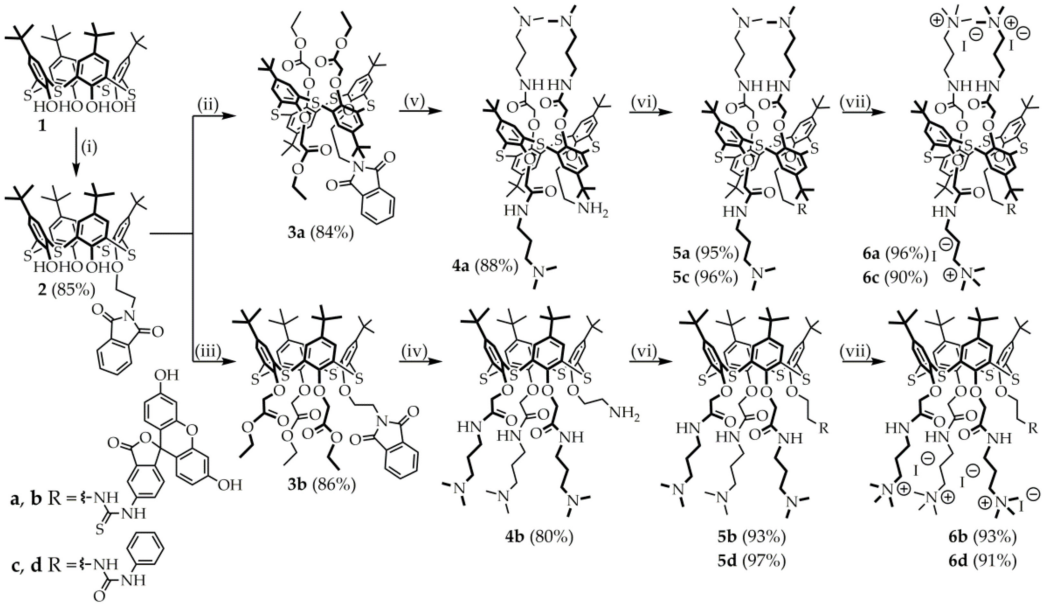

Scheme 1. Reagents and conditions: (**i**) *N*-(2-bromoethyl)phthalimide, Cs_2CO_3, $(CH_3)_2CO$; (**ii**) $BrCH_2CO_2Et$, Cs_2CO_3, $(CH_3)_2CO$; (**iii**) $BrCH_2CO_2Et$, Na_2CO_3, $(CH_3)_2CO$; (**iv**) $NH_2(CH_2)_3N(CH_3)_2$, CH_3OH; (**v**) $NH_2(CH_2)_3N(CH_3)_2$; (**vi**) FITC or PhIC, DMF; (**vii**) CH_3I, CH_3OH.

Further, the possibility of the aminolysis of the obtained compounds **3a**–**b** with *N*,*N*-dimethylpropanediamine was studied. The use of heating led to an inversion of the conformations of the final products, and therefore, the reaction was carried out at room temperature for 70 h in methanol. Analysis of the ^{1}H NMR spectra of the aminolysis products (Figures S1 and S2, ESI) showed no signals from the phthalimide group protons. The isolated aminolysis products are compounds in which the three ester groups of the starting compounds **3a**–**b** reacted with *N*,*N*-dimethylpropanediamine to form amide groups, and the phthalimide group is absent. It was found that the reaction of compounds **3a**–**b** with *N*,*N*-dimethylpropanediamine resulted in both methods, i.e., aminolysis of the ester groups and removal of the phthalimide protection with the formation of a primary amino group. The resulting compounds containing a primary amino group will be used for further functionalization of their various fragments, including fluorescein. Thus, thiacalix[4]arenes **4a**–**b** were obtained in one step from triester derivatives **3a**–**b** (*cone* and *1,3-alternate*) in 80% and 88% yields, respectively (Scheme 1).

It is known [49] that the energy barrier to the inversion of the aryl fragment in thiacalix[4]arenes containing substituents less than four atoms long at the lower rim is low. In this regard, the conformation of compounds **4a**–**b** containing a primary amino group was confirmed by the 2D ^{1}H-^{1}H NOESY NMR spectroscopy. The ^{1}H-^{1}H NOESY NMR spectrum of macrocycle **4a** shows cross peaks between the protons of the *tert*-butyl groups and the methylene group bonded to the nitrogen atom as well as cross-peaks between the protons of the *tert*-butyl and amide groups, which indicates *1,3-alternate* conformation of

thiacalix[4]arene **4a**. In the case of compound **4b** in *cone* conformation, only cross-peaks between protons of *tert*-butyl and aryl groups as well as cross-peaks between protons of the oxymethylene and amide groups are observed (Figures S41 and S42, ESI).

An analysis of the published data showed [50,51] that the optimal way for the covalent introduction of a fluorescent label is the reaction of the primary amino group with the isothiocyanate fragment. Fluorescein isothiocyanate (FITC) is a commercially available reagent. The covalent introduction of FITC into the macrocyclic platform has also been reported [52–54]. Based on previously published methods for the covalent introduction of FITC, we developed our own modified synthesis procedure. Using this procedure, the thiacalix[4]arenes **5a**–**b** (*cone* and *1,3-alternate*) were obtained by reacting compounds **4a**–**b** with FITC in DMF at room temperature in high yields of 93% and 95%, respectively (Scheme 1). The resulting compounds are poorly soluble in water. To increase the water solubility of **5a**–**b**, the Menshutkin alkylation reaction of tertiary amino groups in compounds **5a**–**b** was carried out with iodomethane as one of the most common and highly reactive alkylating agents. As a result, thiacalix[4]arenes **6a**–**b** were isolated in 93% (**6b**, *cone*) and 96% (**6a**, *1,3-alternate*) yields. In order to study the effect of the fluorescein fragment on the final cytotoxicity of macrocycles **5a**–**b** and **6a**–**b**, similar compounds containing one phenylisocyanate (PhIC) fragment, **5c**–**d** and **6c**–**d,** were also synthesized (Scheme 1).

Thus, using the original strategy of regioselective functionalization of the thiacalix[4]arene platform, phenylisocyanate- and fluorescein-containing analogs of drugs **PTX008**–**PTX015** were obtained. All obtained compounds were characterized by ^{1}H and ^{13}C NMR, IR spectroscopy, HRMS (Figures S1–S40, ESI).

3.2. Aggregation Properties of Fluorescein- and Phenyl-Labeled Thiacalix[4]arenes

Before studying the interaction of the synthesized compounds with cells, first of all, it is necessary to answer the question of what form the obtained compounds take in the solution. There are no data on the self-association and aggregation of previously investigated **PTX008**–**PTX015** compounds (Figure 1) in solutions in the literature data and patents. Therefore, the study of the aggregation properties of the compounds synthesized by us is of particular interest. The self-association and aggregation of compounds **6a**–**d** were studied in water by the DLS method (Table 1).

Table 1. Sizes of compounds **6a**–**d** aggregates in water, obtained by the DLS method.

Concentration, M	FITC Derivatives				PhIC Derivatives			
	6a		6b		6c		6d	
	D, nm	PDI	D, nm	PDI	D, nm	PDI	D, nm	PDI
1×10^{-3}	587 ± 35	0.43	329 ± 59	0.57	–	–	–	–
1×10^{-4}	433 ± 43	0.51	353 ± 93	0.64	323 ± 16	0.28	262 ± 38	0.49
1×10^{-5}	285 ± 44	0.44	199 ± 45	0.48	298 ± 32	0.59	185 ± 16	0.29
1×10^{-6}	–	–	–	–	277 ± 34	0.59	186 ± 38	0.42

The study of self-association of compounds **6a**–**b** containing a fluorescein fragment was carried out in water in the concentration range from 1×10^{-3} M to 1×10^{-5} M. Synthesized compounds **6a**–**d** were dissolved completely in deionized water at concentrations used in the research (from 1×10^{-6} M to 1×10^{-3} M). Deionized water with resistivity >18.0 MΩ cm (Millipore-Q) was used for the preparation of the solutions. The temperature of the solutions was maintained at 25 °C during the experiment. It was shown (Table 1) that the macrocycle **6a** (*1,3-alternate*) form self-associates with a larger hydrodynamic diameter (285–587 nm) than the similar macrocycle **6b** (*cone*) (199–353 nm). It should be noted that the solubility of compounds **6c**–**d** containing the phenyl isocyanate fragment is lower than the water solubility of compounds **6a**–**b**. The concentration range from 1×10^{-4} M to 1×10^{-6} M was used to study compounds **6c**–**d** in water by the DLS method. The average

hydrodynamic diameter of self-associates formed by the macrocycle **6c** (*1,3-alternate*) is larger (277–323 nm) than that of the similar macrocycle **6d** (*cone*) (185–262 nm).

Thus, we can conclude that macrocycles **6a–d** interact with cells as supramolecular self-associates.

3.3. Cytotoxicity of Synthesized Macrocycles

A series of experiments were performed using the *A549* human lung adenocarcinoma cell line (which actively expresses galectin-1 [55]) and the *HuTu-80* human duodenal adenocarcinoma cell line. The ability of **6a–d** to inhibit the cells' viability and proliferative activity was determined using the MTT test [48] after incubation for 24 h. It was found that **6a** and **6c** (*1,3-alternate*) did not reduce the viability of *A549* cells over the entire range of concentrations studied (0.5–100 μg/mL) (Figure 2). It was also shown that **6b** and **6d** (*cone*) had a cytotoxic effect on *A549* cells at concentrations of ≥50 μg/mL (**6b**) and ≥25 μg/mL (**6d**) (Figure 2).

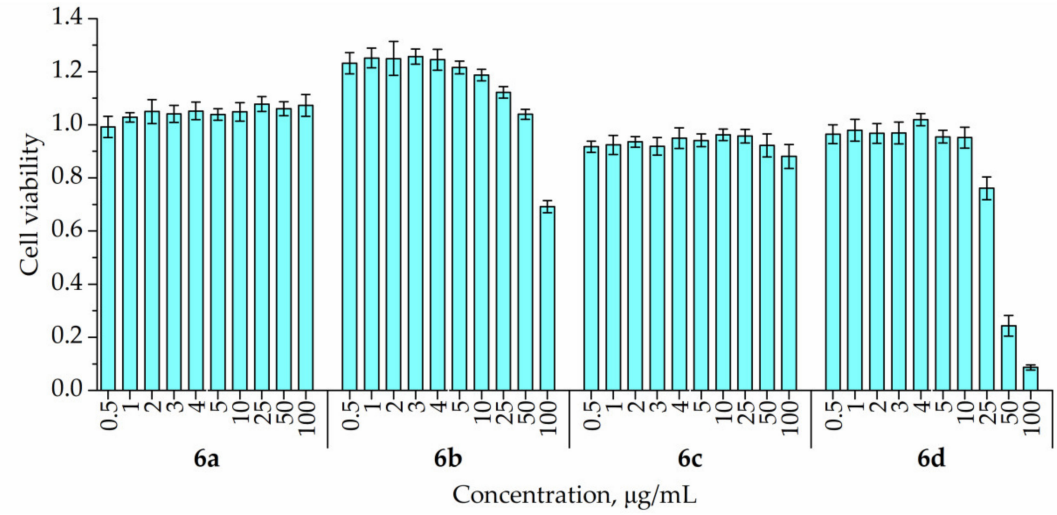

Figure 2. Cytotoxicity of compounds **6a–d** on cell line *A549*.

Experiments with the *HuTu-80* cell line showed that compound **6a** (*1,3-alternate)* did not have the ability to reduce the viability of *HuTu-80* cells at a concentration of ≤50 μg/mL (Figure 3). The cytotoxic activity of compound **6a** was fixed at the concentration of 100 μg/mL, and the viability of *HuTu-80* cells after treatment with **6a** was 0.67 ± 0.05. The macrocycles **6b** (*cone*) and **6c** (*1,3-alternate*) were cytotoxic to *HuTu-80* cells at concentrations ≥ 25 μg/mL (Figure 3). The cytotoxic effect of **6d** (*cone*) was negligible at concentrations ≤4 μg/mL (Figure 3). Exposure to compound **6d** increased with the increasing concentration and was significant at concentrations 50 μg/mL or more. At concentrations above 50 μg/mL, **6d** almost completely eliminated *HuTu-80* cells.

The results of the analysis of the cytotoxic activity of macrocyclic compounds in relation to *HuTu-80* cells correspond to the data obtained in relation to *A549* cells. It was shown that the cell line *HuTu-80* was more sensitive to the effects of these substances. For all studied samples of macrocyclic compounds, the average inhibitory concentration (IC_{50}) was calculated (Table 2). Summarizing the presented data, thiacalix[4]arenes **6a** and **6c** (*1,3-alternate*) did not have a strong toxic effect. The IC_{50} value of substance **6b** (*cone*) for *HuTu-80* cells was 49.11 μg/mL. Compound **6d** (*cone*) was shown to have the highest toxic properties, with IC_{50} 21.83 μg/mL and 37.55 μg/mL for *HuTu-80* and *A549* cells, correspondingly (Table 2). Thus, the conformation of trisubstituted macrocycles affects their cytotoxicity; as a rule, compounds in *cone* conformation are more toxic than macrocycles in *1,3-alternate* conformation.

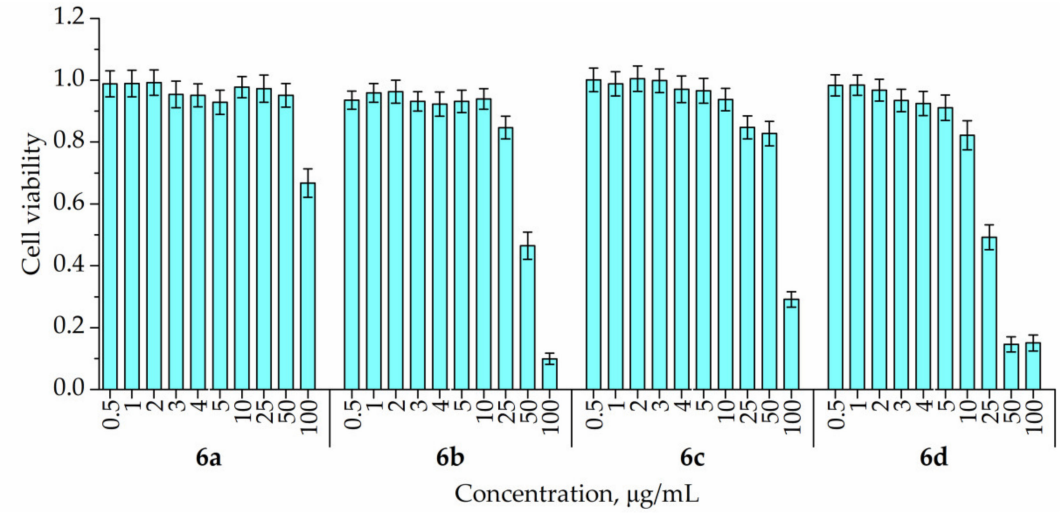

Figure 3. Cytotoxicity of compounds **6a–d** on cell line *HuTu-80*.

Table 2. IC_{50} values of the macrocycles.

Compounds	IC_{50}, μg/mL	
	HuTu-80	***A549***
6a (*1,3-alternate*)	>100 [a]	>100 [a]
6b (*cone*)	49.11	>100 [a]
6c (*1,3-alternate*)	>100 [a]	>100 [a]
6d (*cone*)	21.83	37.55
PTX008 (*cone*)	nd	1.87 [b]
PTX013 (*cone*)	nd	0.87 [b]
PTX014 (*cone*)	nd	8.28 [b]

[a] IC_{50} have not been reached in the studied concentration range. [b] Data from literary sources [22] "nd" indicates no data.

We can conclude that FITC-containing compound **6b** (*cone*) has a lower toxic effect compared to the similar PhIC-containing compound **6d** (*cone*) both on *A549* and *HuTu-80* cells (Table 2). Apparently, the size of the macrocycle affects the efficiency of the interaction of the compound with the cell. If we compare the toxic effect of compounds **6a–d** with similar compounds based on tetrasubstituted macrocycles (in *cone* conformations) **PTX008–PTX015** (Table 2), we can see that the trisubstituted compounds have a lower toxic effect. Apparently, this is due to the inhibition of galectin, which is carried out by terminal amino groups. Thus, four fragments of tetrasubstituted calixarenes inhibit galectin more efficiently, unlike three fragments in compounds **6b** and 6**d**. This assumption correlates with previously published data on the putative mechanism of the cytotoxic effect of **PTX008–PTX015** [22].

Thus, the antiproliferative and cytotoxic activity of synthesized compounds **6a–d** as analogs of the anti-angiogenic agents were evaluated. It was found that macrocycles **6b,d** (*cone*) are more cytotoxic than macrocycles **6a,c** (*1,3-alternate)*. However, the cytotoxicity of the obtained compounds is lower than similar **PTX008–PTX015** compounds, which is explained by the smaller number of terminal amino groups and correlates with the proposed mechanism of action of **PTX008–PTX015** compounds [22].

3.4. Penetration into A549 and HuTu-80 Cells of Synthesized Macrocycles

The next step of the work was to determine the ability of macrocyclic compounds **6a–d** to penetrate into *A549* and *HuTu-80* cells using flow cytometry with propidium iodide co-staining. It was found that associates of compounds **6a–d** after 2 h of incubation penetrate into both living and dead *A549* and *HuTu-80* cells (Figure 4), and the penetrating ability of

thiacalix[4]arenes is quite high. It should be noted that **6a–d**, when incubated with cells, had a toxic effect on both *A549* and *HuTu-80* cells. The proportion of dead cells in the population in the presence of **6a–d** increased significantly. The cytotoxicity of the studied compounds **6a–d** depended on the concentration and reached the highest values for agent concentrations of 100 μg/mL. In this study, thiacalix[4]arenes can be ranked according to the cytotoxicity exerted on *A549* cells in the order **6a** → **6c** → **6b** → **6d**. It can be noted that the macrocycles **6b** and **6d** (*cone*) had a higher toxic effect on *A549* cells than macrocycles **6a** and **6c** (*1,3-alternate*). Compound **6a** had the worst penetrating ability, staining only 36.6% and 61% of *A549* cells at concentrations of 5 μg/mL and 10 μg/mL, respectively. On the *HuTu-80* cell line, thiacalix[4]arenes can be ranked by increasing cytotoxicity in the order **6c** → **6a** → **6b** → **6d**. It can be noted that both in the case of the *A549* cell line and in the case of the *HuTu-80* cell line, macrocycles **6b** and **6d** (*cone*) had a higher toxic effect on cells than macrocycles **6a** and **6c** (*1,3-alternate*). At concentrations of 5 μg/mL and 10 μg/mL, all tested compounds stained only up to 50% of the *HuTu-80* cells.

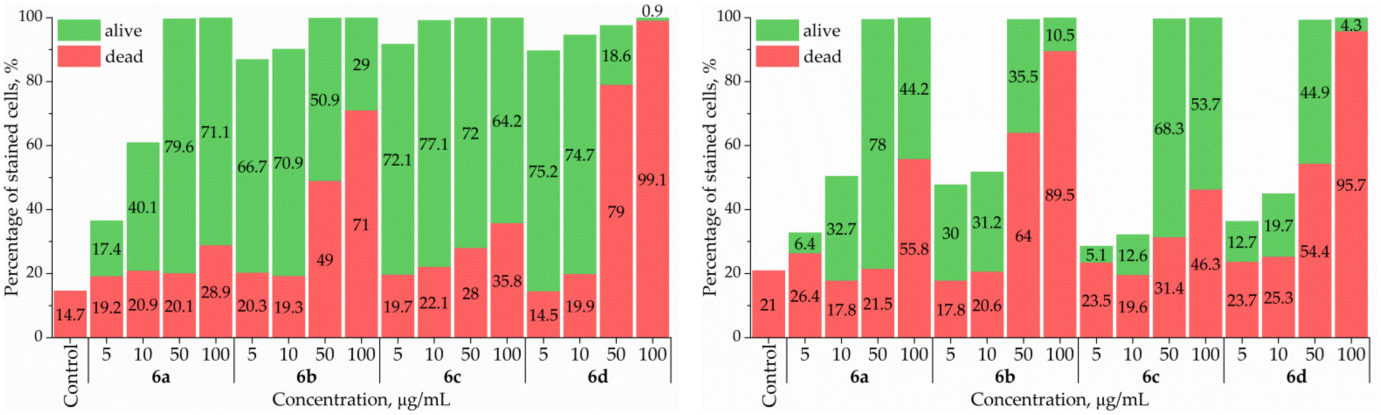

Figure 4. Penetration of thiacalix[4]arenes **6a–d** into *A549* (**a**) and *HuTu-80* (**b**) cells.

The ability of macrocycles **6a–d** to penetrate into *A549* and *HuTu-80* cell lines was evaluated. In conclusion, one can say that macrocycles penetrate into living and dead cells; the cytometric cytotoxic profiles confirm the MTT test data.

4. Conclusions

Thus, an approach to create potential theranostic molecules with both a pharmacophore fragment and a fluorescent fragment was proposed and implemented. Phenylisocyanate- and fluorescein-containing analogs of antiangiogenic agents **PTX008–PTX015** were obtained by the original regioselective method of the functionalization of thiacalix[4]arene. All obtained compounds were characterized by ^{1}H, ^{13}C NMR, IR spectroscopy, and HRMS. Using the DLS method, it was established that the synthesized macrocycles form self-associates only in aqueous solutions with average hydrodynamic diameters of 166–465 nm. The antiproliferative and cytotoxic activity of the synthesized compounds **6a–d** (analogs of the anti-angiogenic agents **PTX008–PTX015**) was evaluated by the MTT test and confirmed cytometrically. It was found that macrocycles **6b,d** (*cone*) are more cytotoxic than macrocycles **6a,c** (*1,3-alternate*). It was also shown that macrocycles can penetrate both living and dead *A549* and *HuTu-80* cancer cells. The resulting macrocycles are potential theranostic molecules that combine both the pharmacophore fragment for the treatment of tumor neoplasms and the fluorescent fragment for monitoring the delivery and biodistribution of nanomedicines.

Supplementary Materials: The following supporting information can be downloaded at: https://www.mdpi.com/article/10.3390/pharmaceutics14112340/s1, Characterization of compounds **4a–b**, **5a–d**, **6a–d**; Figures S1–S10. 1H NMR spectra of compounds **4a–b, 5a–d, 6a–d**; Figures S11–S20. 13C NMR spectra of compounds **4a–b, 5a–d, 6a–d**; Figures S21–S30. FT-IR spectra of compounds **4a–b, 5a–d, 6a–d**; Figures S31–S40. HRMS spectra of compounds **4a–b, 5a–d, 6a–d**; Figures S41 and S42 ^{1}H-^{1}H NOESY spectra of compounds **4a–b**.

Author Contributions: Conceptualization, writing—review and editing, supervision, I.S.; investigation, writing—original draft and visualization, A.A.; data curation and supervision P.P., P.Z., and D.S.; investigation, O.T., E.S. and R.S.; funding acquisition, P.P. All authors have read and agreed to the published version of the manuscript.

Funding: This work was financially supported by Russian Science Foundation, Russian Federation (project number 19-73-10134, https://rscf.ru/en/project/19-73-10134/).

Institutional Review Board Statement: Not applicable.

Informed Consent Statement: Not applicable.

Data Availability Statement: The data presented in this study are available in the Supplementary Material.

Acknowledgments: The investigation of the spatial structure of the compounds by NMR spectroscopy was supported by the Kazan Federal University Strategic Academic Leadership Program ('PRIORITY–2030').

Conflicts of Interest: The authors declare no conflict of interest. The funders had no role in the design of the study; in the collection, analyses, or interpretation of data; in the writing of the manuscript, or in the decision to publish the results.

References

1. Sung, H.; Ferlay, J.; Siegel, R.L.; Laversanne, M.; Soerjomataram, I.; Jemal, A.; Bray, F. Global Cancer Statistics 2020: GLOBOCAN Estimates of Incidence and Mortality Worldwide for 36 Cancers in 185 Countries. *CA A Cancer J. Clin.* **2021**, *71*, 209–249. [CrossRef] [PubMed]
2. Ling, A.; Lundberg, I.V.; Eklöf, V.; Wikberg, M.L.; Öberg, Å.; Edin, S.; Palmqvist, R. The Infiltration, and Prognostic Importance, of Th1 Lymphocytes Vary in Molecular Subgroups of Colorectal Cancer. *J. Path. Clin. Res.* **2015**, *2*, 21–31. [CrossRef] [PubMed]
3. Amicarella, F.; Muraro, M.G.; Hirt, C.; Cremonesi, E.; Padovan, E.; Mele, V.; Governa, V.; Han, J.; Huber, X.; Droeser, R.A.; et al. Dual Role of Tumour-Infiltrating T Helper 17 Cells in Human Colorectal Cancer. *Gut* **2015**, *66*, 692–704. [CrossRef] [PubMed]
4. Thijssen, V.L.; Heusschen, R.; Caers, J.; Griffioen, A.W. Galectin Expression in Cancer Diagnosis and Prognosis: A Systematic Review. *Biochim. Et Biophys. Acta (BBA) Rev. Cancer* **2015**, *1855*, 235–247. [CrossRef]
5. Rabinovich, G.A.; Conejo-García, J.R. Shaping the Immune Landscape in Cancer by Galectin-Driven Regulatory Pathways. *J. Mol. Biol.* **2016**, *428*, 3266–3281. [CrossRef]
6. Chang, W.; Tsai, M.; Kuo, P.; Hung, J. Role of Galectins in Lung Cancer (Review). *Oncol. Lett.* **2017**, *14*, 5077–5084. [CrossRef]
7. Chou, F.-C.; Chen, H.-Y.; Kuo, C.-C.; Sytwu, H.-K. Role of Galectins in Tumors and in Clinical Immunotherapy. *Int. J. Mol. Sci.* **2018**, *19*, 430. [CrossRef]
8. Huang, Y.; Wang, H.-C.; Zhao, J.; Wu, M.-H.; Shih, T.-C. Immunosuppressive Roles of Galectin-1 in the Tumor Microenvironment. *Biomolecules* **2021**, *11*, 1398. [CrossRef]
9. Sanjuan, X.; Fernandez, P.; Castells, A.; Castronovo, V.; van den Brule, F.; Liu, F.; Cardesa, A.; Campo, E. Differential Expression of Galectin 3 and Galectin 1 in Colorectal Cancer Progression. *Gastroenterology* **1997**, *113*, 1906–1915. [CrossRef]
10. Blair, B.B.; Funkhouser, A.T.; Goodwin, J.L.; Strigenz, A.M.; Chaballout, B.H.; Martin, J.C.; Arthur, C.M.; Funk, C.R.; Edenfield, W.J.; Blenda, A.V. Increased Circulating Levels of Galectin Proteins in Patients with Breast, Colon, and Lung Cancer. *Cancers* **2021**, *13*, 4819. [CrossRef]
11. Spano, D.; Russo, R.; Di Maso, V.; Rosso, N.; Terracciano, L.M.; Roncalli, M.; Tornillo, L.; Capasso, M.; Tiribelli, C.; Iolascon, A. Galectin-1 and Its Involvement in Hepatocellular Carcinoma Aggressiveness. *Mol. Med.* **2009**, *16*, 102–115. [CrossRef] [PubMed]
12. Fanfone, D.; Stanicki, D.; Nonclercq, D.; Port, M.; Vander Elst, L.; Laurent, S.; Muller, R.N.; Saussez, S.; Burtea, C. Molecular Imaging of Galectin-1 Expression as a Biomarker of Papillary Thyroid Cancer by Using Peptide-Functionalized Imaging Probes. *Biology* **2020**, *9*, 53. [CrossRef]
13. Chen, R.; Pan, S.; Ottenhof, N.A.; de Wilde, R.F.; Wolfgang, C.L.; Lane, Z.; Post, J.; Bronner, M.P.; Willmann, J.K.; Maitra, A.; et al. Stromal Galectin-1 Expression Is Associated with Long-Term Survival in Resectable Pancreatic Ductal Adenocarcinoma. *Cancer Biol. Ther.* **2012**, *13*, 899–907. [CrossRef] [PubMed]

14. Kuo, P.-L.; Hung, J.-Y.; Huang, S.-K.; Chou, S.-H.; Cheng, D.-E.; Jong, Y.-J.; Hung, C.-H.; Yang, C.-J.; Tsai, Y.-M.; Hsu, Y.-L.; et al. Lung Cancer-Derived Galectin-1 Mediates Dendritic Cell Anergy through Inhibitor of DNA Binding 3/IL-10 Signaling Pathway. *J. Immunol.* **2010**, *186*, 1521–1530. [CrossRef] [PubMed]
15. Abroun, S.; Otsuyama, K.; Shamsasenjan, K.; Islam, A.; Amin, J.; Iqbal, M.S.; Gondo, T.; Asaoku, H.; Kawano, M.M. Galectin-1 Supports the Survival of CD45RA(−) Primary Myeloma Cellsin Vitro. *Br. J. Haematol.* **2008**, *142*, 754–765. [CrossRef]
16. Croci, D.O.; Cerliani, J.P.; Pinto, N.A.; Morosi, L.G.; Rabinovich, G.A. Regulatory Role of Glycans in the Control of Hypoxia-Driven Angiogenesis and Sensitivity to Anti-Angiogenic Treatment. *Glycobiology* **2014**, *24*, 1283–1290. [CrossRef]
17. Astorgues-Xerri, L.; Riveiro, M.E.; Tijeras-Raballand, A.; Serova, M.; Neuzillet, C.; Albert, S.; Raymond, E.; Faivre, S. Unraveling Galectin-1 as a Novel Therapeutic Target for Cancer. *Cancer Treat. Rev.* **2014**, *40*, 307–319. [CrossRef]
18. Blanchard, H.; Bum-Erdene, K.; Bohari, M.H.; Yu, X. Galectin-1 Inhibitors and Their Potential Therapeutic Applications: A Patent Review. *Expert Opin. Ther. Pat.* **2016**, *26*, 537–554. [CrossRef]
19. Berzenji, L.; Van Schil, P. Multimodality Treatment of Malignant Pleural Mesothelioma. *F1000Research* **2018**, *7*, 1681. [CrossRef]
20. Mayo, K.H.; van der Schaft, D.W.J.; Griffioen, A.W. Designed β-sheet peptides that inhibit proliferation and induce apoptosis in endothelial cells. *Angiogenesis* **2001**, *4*, 45–51. [CrossRef]
21. Dings, R.P.M.; Chen, X.; Hellebrekers, D.M.E.I.; van Eijk, L.I.; Zhang, Y.; Hoye, T.R.; Griffioen, A.W.; Mayo, K.H. Design of Nonpeptidic Topomimetics of Antiangiogenic Proteins With Antitumor Activities. *JNCI J. Natl. Cancer Inst.* **2006**, *98*, 932–936. [CrossRef] [PubMed]
22. Dings, R.P.M.; Levine, J.I.; Brown, S.G.; Astorgues-Xerri, L.; MacDonald, J.R.; Hoye, T.R.; Raymond, E.; Mayo, K.H. Polycationic Calixarene PTX013, a Potent Cytotoxic Agent against Tumors and Drug Resistant Cancer. *Invest. New Drugs* **2013**, *31*, 1142–1150. [CrossRef] [PubMed]
23. Kevin, H.M.; Thomas, R.H.; Chen, X. Calixarene-Based Peptide Conformation Mimetics, Methods of Use, and Methods of Making. U.S. Patent 8716343B2, 6 December 2012. International filing date: 24 April 2012.
24. Dings, R.P.M.; Miller, M.C.; Nesmelova, I.; Astorgues-Xerri, L.; Kumar, N.; Serova, M.; Chen, X.; Raymond, E.; Hoye, T.R.; Mayo, K.H. Antitumor Agent Calixarene 0118 Targets Human Galectin-1 as an Allosteric Inhibitor of Carbohydrate Binding. *J. Med. Chem.* **2012**, *55*, 5121–5129. [CrossRef] [PubMed]
25. Yu, G.; Chen, X. Host-Guest Chemistry in Supramolecular Theranostics. *Theranostics* **2019**, *9*, 3041–3074. [CrossRef]
26. Shurpik, D.N.; Padnya, P.L.; Stoikov, I.I.; Cragg, P.J. Antimicrobial Activity of Calixarenes and Related Macrocycles. *Molecules* **2020**, *25*, 5145. [CrossRef]
27. Padnya, P.L.; Terenteva, O.S.; Akhmedov, A.A.; Iksanova, A.G.; Shtyrlin, N.V.; Nikitina, E.V.; Krylova, E.S.; Shtyrlin, Y.G.; Stoikov, I.I. Thiacalixarene Based Quaternary Ammonium Salts as Promising Antibacterial Agents. *Bioorganic Med. Chem.* **2021**, *29*, 115905. [CrossRef]
28. Shurpik, D.N.; Sevastyanov, D.A.; Zelenikhin, P.V.; Padnya, P.L.; Evtugyn, V.G.; Osin, Y.N.; Stoikov, I.I. Nanoparticles Based on the Zwitterionic Pillardoi:5Arene and Ag^+: Synthesis, Self-Assembly and Cytotoxicity in the Human Lung Cancer Cell Line A549. *Beilstein J. Nanotechnol* **2020**, *11*, 421–431. [CrossRef]
29. Akhmedov, A.A.; Shurpik, D.N.; Padnya, P.L.; Khadieva, A.I.; Gamirov, R.R.; Panina, Y.V.; Gazizova, A.F.; Grishaev, D.Y.; Plemenkov, V.V.; Stoikov, I.I. Supramolecular Amphiphiles Based on Pillardoi:5Arene and Meroterpenoids: Synthesis, Self-Association and Interaction with Floxuridine. *Int. J. Mol. Sci.* **2021**, *22*, 7950. [CrossRef]
30. Shurpik, D.N.; Akhmedov, A.A.; Cragg, P.J.; Plemenkov, V.V.; Stoikov, I.I. Progress in the Chemistry of Macrocyclic Meroterpenoids. *Plants* **2020**, *9*, 1582. [CrossRef]
31. Shurpik, D.N.; Aleksandrova, Y.I.; Mostovaya, O.A.; Nazmutdinova, V.A.; Tazieva, R.E.; Murzakhanov, F.F.; Gafurov, M.R.; Zelenikhin, P.V.; Subakaeva, E.V.; Sokolova, E.A.; et al. Self-Healing Thiolated Pillardoi:5Arene Films Containing Moxifloxacin Suppress the Development of Bacterial Biofilms. *Nanomaterials* **2022**, *12*, 1604. [CrossRef]
32. Shurpik, D.N.; Aleksandrova, Y.I.; Rodionov, A.A.; Razina, E.A.; Gafurov, M.R.; Vakhitov, I.R.; Evtugyn, V.G.; Gerasimov, A.V.; Kuzin, Y.I.; Evtugyn, G.A.; et al. Metallo-Supramolecular Coordination Polymers Based on Amidopyridine Derivatives of Pillardoi:5Arene and Cu(II) and Pd(II) Cations: Synthesis and Recognition of Nitroaromatic Compounds. *Langmuir* **2021**, *37*, 2942–2953. [CrossRef] [PubMed]
33. Akhmedov, A.; Shurpik, D.; Latypova, Z.; Gamirov, R.; Plemenkov, V.; Stoikov, I. A Synthetic Analogue of Archaea Lipids Based on Aminoglycerin and Geraniol: Synthesis and Membranotropic Properties. In Proceedings of the International Scientific Conference Actual Problems of Organic Chemistry and Biotechnology, Ekaterinburg, Russia, 18–21 November 2020; p. 69473. [CrossRef]
34. Lebrón, J.A.; López-López, M.; Moyá, M.L.; Deasy, M.; Muñoz-Wic, A.; García-Calderón, C.B.; Valle Rosado, I.; López-Cornejo, P.; Bernal, E.; Ostos, F.J. Fluorescent Calixarene-Schiff as a Nanovehicle with Biomedical Purposes. *Chemosensors* **2022**, *10*, 281. [CrossRef]
35. Bahojb Noruzi, E.; Shaabani, B.; Geremia, S.; Hickey, N.; Nitti, P.; Kafil, H.S. Synthesis, Crystal Structure, and Biological Activity of a Multidentate Calix[4]Arene Ligand Doubly Functionalized by 2-Hydroxybenzeledene-Thiosemicarbazone. *Molecules* **2020**, *25*, 370. [CrossRef] [PubMed]
36. Oguz, M.; Yildirim, A.; Durmus, I.M.; Karakurt, S.; Yilmaz, M. Synthesis of New Calix[4]Arene Derivatives and Evaluation of Their Cytotoxic Activity. *Med. Chem. Res.* **2021**, *31*, 52–59. [CrossRef]

37. Oguz, M. Synthesis and Anticancer Activity of New P-Tertbutylcalix[4]Arenes Integrated with Trifluoromethyl Aniline Groups against Several Cell Lines. *Tetrahedron* **2022**, *116*, 132816. [CrossRef]
38. Sargazi, S.; Hajinezhad, M.R.; Rahdar, A.; Zafar, M.N.; Awan, A.; Baino, F. Assessment of SnFe2O4 Nanoparticles for Potential Application in Theranostics: Synthesis, Characterization, In Vitro, and In Vivo Toxicity. *Materials* **2021**, *14*, 825. [CrossRef]
39. Redrado, M.; Fernández-Moreira, V.; Gimeno, M.C. Theranostics Through the Synergistic Cooperation of Heterometallic Complexes. *ChemMedChem* **2021**, *16*, 932–941. [CrossRef]
40. Bildziukevich, U.; Kvasnicová, M.; Šaman, D.; Rárová, L.; Wimmer, Z. Novel Oleanolic Acid-Tryptamine and -Fluorotryptamine Amides: From Adaptogens to Agents Targeting In Vitro Cell Apoptosis. *Plants* **2021**, *10*, 2082. [CrossRef]
41. Isik, A.; Oguz, M.; Kocak, A.; Yilmaz, M. Calixarenes: Recent Progress in Supramolecular Chemistry for Application in Cancer Therapy. *J. Incl. Phenom. Macrocycl. Chem.* **2022**, *102*, 439–449. [CrossRef]
42. Pan, Y.; Hu, X.; Guo, D. Biomedical Applications of Calixarenes: State of the Art and Perspectives. *Angew. Chem. Int. Ed.* **2020**, *60*, 2768–2794. [CrossRef]
43. Wang, Y.; Zhang, Z.; Zhao, X.; Xu, L.; Zheng, Y.; Li, H.-B.; Guo, D.-S.; Shi, L.; Liu, Y. Calixarene-Modified Albumin for Stoichiometric Delivery of Multiple Drugs in Combination-Chemotherapy. *Theranostics* **2022**, *12*, 3747–3757. [CrossRef] [PubMed]
44. Nosov, R.V.; Stoikov, I.I. Pentakis-Amidothiacalix[4]Arene Stereoisomers: Synthesis and Effect of Central Core Conformation on Their Aggregation Properties. *MHC* **2015**, *8*, 120–127. [CrossRef]
45. Stoikov, I.I.; Galukhin, A.V.; Zaikov, E.N.; Antipin, I.S. Synthesis and Complexation Properties of 1,3-Alternate Stereoisomers of *p-Tert*-Butylthiacalix[4]Arenes Tetrasubstituted at the Lower Rim by the Phthalimide Group. *Mendeleev Commun.* **2009**, *19*, 193–195. [CrossRef]
46. Kumagai, H.; Hasegawa, M.; Miyanari, S.; Sugawa, Y.; Sato, Y.; Hori, T.; Ueda, S.; Kamiyama, H.; Miyano, S. Facile Synthesis of P-Tert-Butylthiacalix[4]Arene by the Reaction of p-Tert-Butylphenol with Elemental Sulfur in the Presence of a Base. *Tetrahedron Lett.* **1997**, *38*, 3971–3972. [CrossRef]
47. Andreyko, E.A.; Puplampu, J.B.; Ignacio-De Leon, P.A.; Zharov, I.; Stoikov, I.I. P-Tert-Butylthiacalix[4]Arenes Containing Guanidinium Groups: Synthesis and Self-Assembly into Nanoscale Aggregates. *Supramol. Chem.* **2019**, *31*, 473–483. [CrossRef]
48. Mosmann, T. Rapid Colorimetric Assay for Cellular Growth and Survival: Application to Proliferation and Cytotoxicity Assays. *J. Immunol. Methods* **1983**, *65*, 55–63. [CrossRef]
49. Iki, N.; Narumi, F.; Fujimoto, T.; Morohashi, N.; Miyano, S. Selective Synthesis of Three Conformational Isomers of Tetrakis-doi:(Ethoxycarbonyl)MethoxyThiacalix[4]Arene and Their Complexation Properties towards Alkali Metal Ions†. *J. Chem. Soc. Perkin Trans.* **1998**, *2*, 2745–2750. [CrossRef]
50. Baumann, S.; Schoof, S.; Bolten, M.; Haering, C.; Takagi, M.; Shin-ya, K.; Arndt, H.-D. Molecular Determinants of Microbial Resistance to Thiopeptide Antibiotics. *J. Am. Chem. Soc.* **2010**, *132*, 6973–6981. [CrossRef]
51. Miao, S.; Liang, Y.; Marathe, I.; Mao, J.; DeSantis, C.; Bong, D. Duplex Stem Replacement with BPNA+ Triplex Hybrid Stems Enables Reporting on Tertiary Interactions of Internal RNA Domains. *J. Am. Chem. Soc.* **2019**, *141*, 9365–9372. [CrossRef]
52. Shurpik, D.N.; Aleksandrova, Y.I.; Mostovaya, O.A.; Nazmutdinova, V.A.; Zelenikhin, P.V.; Subakaeva, E.V.; Mukhametzyanov, T.A.; Cragg, P.J.; Stoikov, I.I. Water-Soluble Pillardoi:5Arene Sulfo-Derivatives Self-Assemble into Biocompatible Nanosystems to Stabilize Therapeutic Proteins. *Bioorganic Chem.* **2021**, *117*, 105415. [CrossRef]
53. Sharma, N.; Reja, S.I.; Bhalla, V.; Kumar, M. A New Thiacalix[4]Arene-Fluorescein Based Probe for Detection of CN^- and Cu^{2+} Ions and Construction of a Sequential Logic Circuit. *Dalton Trans.* **2014**, *43*, 15929–15936. [CrossRef] [PubMed]
54. Kumar, R.; Sharma, A.; Singh, H.; Suating, P.; Kim, H.S.; Sunwoo, K.; Shim, I.; Gibb, B.C.; Kim, J.S. Revisiting Fluorescent Calixarenes: From Molecular Sensors to Smart Materials. *Chem. Rev.* **2019**, *119*, 9657–9721. [CrossRef] [PubMed]
55. Zhang, L.; Liu, X.; Tang, Z.; Li, X.; Wang, G. Reversal of Galectin-1 Gene Silencing on Resistance to Cisplatin in Human Lung Adenocarcinoma A549 Cells. *Biomed. Pharmacother.* **2016**, *83*, 265–270. [CrossRef] [PubMed]